Journal of Orthopaedic Translation 40 (2023) 72–79

Contents lists available at ScienceDirect

Journal of Orthopaedic Translation

journal homepage: www.journals.elsevier.com/journal-of-orthopaedic-translation

Original Article

Platelet-derived extracellular vesicles formulated with hyaluronic acid gels for application at the bone-implant interface: An animal study

Miquel Antich-Rosselló [a,b], Maria Antònia Forteza-Genestra [a,b], Hans Jacob Ronold [c], Staale Petter Lyngstadaas [d], Mario García-González [e], María Permuy [f], Mónica López-Peña [e,f], Fernando Muñoz [e,f], Marta Monjo [a,b,g,**], Joana M. Ramis [a,b,g,*]

[a] Cell Therapy and Tissue Engineering Group, Research Institute on Health Sciences (IUNICS), University of the Balearic Islands (UIB), Ctra. Valldemossa Km 7.5, 07122, Palma, Spain
[b] Health Research Institute of the Balearic Islands (IdISBa), Palma, Spain
[c] Department of Prosthetic Dentistry, Institute of Clinical Dentistry, University of Oslo, Oslo, Norway
[d] Department of Biomaterials, Institute of Clinical Dentistry, University of Oslo, Oslo, Norway
[e] Departamento de Ciencias Clínicas Veterinarias. Universidade de Santiago de Compostela. Campus Universitario S/n, 27002, Lugo, Spain
[f] IBoneLab SL, Avenida da Coruña 500; 27003, Lugo, Spain
[g] Departament de Biologia Fonamental I Ciències de La Salut, UIB, Palma, Spain

ARTICLE INFO

Keywords:
Extracellular vesicles
Platelets
Hyaluronic acid
Bone regeneration
Titanium implants

ABSTRACT

Background/Objective: Platelet derived extracellular vesicles (pEV) are promising therapeutical tools for bone healing applications. In fact, several *in vitro* studies have already demonstrated the efficacy of Extracellular Vesicles (EV) in promoting bone regeneration and repair in various orthopedic models. Therefore, to evaluate the translational potential in this field, an *in vivo* study was performed.

Methods: Here, we used hyaluronic acid (HA) gels formulated with pEVs, as a way to directly apply pEVs and retain them at the bone defect. In this study, pEVs were isolated from Platelet Lysate (PL) through size exclusion chromatography and used to formulate 2% HA gels. Then, the gels were locally applied on the tibia cortical bone defect of New Zeland White rabbits before the surgical implantation of coin-shaped titanium implants. After eight weeks, the bone healing process was analyzed through biomechanical, micro-CT, histological and biochemical analysis.

Results: Although no biomechanical differences were observed between pEV formulated gels and non-formulated gels, biochemical markers of the wound fluid at the interface presented a decrease in Lactate dehydrogenase (LDH) activity and alkaline phosphatase (ALP) activity for pEV HA treated implants. Moreover, histological analyses showed that none of the treatments induced an irritative effect and, a decrease in the fibrotic response surrounding the implant for pEV HA treated implants was described.

Conclusion: In conclusion, pEVs improve titanium implants biocompatibility at the bone–implant interface, decreasing the necrotic effects of the surgery and diminishing the fibrotic layer associated to the implant encapsulation that can lead to implant failure.

The translational potential of this article

Human pEVs are good candidates for orthopedic application and could improve the biocompatibility of current treatments. Overall, pEVs could be available in many blood biobanks and they could be used for regenerative medicine purposes.

1. Introduction

Extracellular Vesicles (EV) use for medical applications has been

* Corresponding author. Cell Therapy and Tissue Engineering Group, Research Institute on Health Sciences (IUNICS), University of the Balearic Islands (UIB), Ctra. Valldemossa Km 7.5, 07122, Palma, Spain.
** Corresponding author. Cell Therapy and Tissue Engineering Group, Research Institute on Health Sciences (IUNICS), University of the Balearic Islands (UIB), Ctra. Valldemossa Km 7.5, 07122, Palma, Spain.
E-mail addresses: marta.monjo@uib.es (M. Monjo), joana.ramis@uib.es (J.M. Ramis).

https://doi.org/10.1016/j.jot.2023.05.009
Received 27 February 2023; Received in revised form 5 May 2023; Accepted 30 May 2023
Available online 10 June 2023

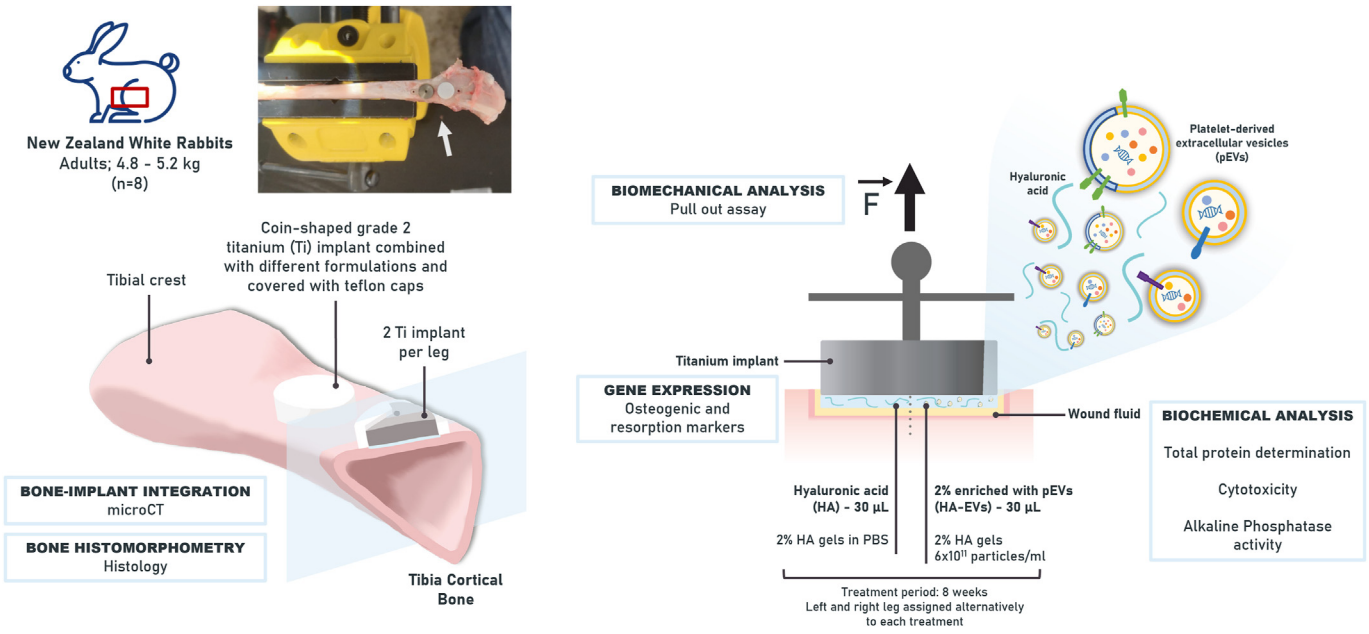

Fig. 1. Animal model set-up. (a) Schematic representation of Ti implants on tibial cortical bone with HA-EV treatment. **(b)** Image of the extracted bone with the two implants attached. **(c)** Schematic representation of the implant extraction and the analyses performed to the extracted implant and to the wound fluid. **(d)** Histological and micro-CT analyses of the samples with non-extracted implants.

extensively reported [1], being most of the studies mainly focused on stem cell or immune cells derived EVs [2,3]. Nonetheless, platelet concentrates are another regenerative source that bring high expectations [4–6], having platelet derived extracellular vesicles (pEVs) also emerged as great candidates in the regenerative medicine field [7].

More concretely, the use of pEVs is especially interesting for bone healing, since several *in vitro* studies have reported osteogenic effects [8,9]. Moreover, pEVs are known to prevent apoptosis and to induce proliferation in osteonecrosis induced osteoblasts [10]. These effects have been associated to their miRNA and protein content, including growth factors [8,11]. In addition, pEVs are immunomodulators [12] and they can also induce angiogenic responses [13], which are both necessary for tissue repair.

Furthermore, pEVs can also be combined with biomaterials to achieve more applicable medical devices for bone tissue engineering. Among the different biomaterials available, titanium (Ti) is widely used in clinics because of its mechanical properties and biocompatibility [14]. Therefore, some studies have already used cell-derived EVs to coat titanium surfaces [15–19]. However, direct functionalization of titanium with EVs can modulate their initial functional effects [20]. These changes are related to the heterogeneity of the EV samples, since there are different EV subpopulations depending on their size, morphology, composition and cellular origin, having each specific functional effects [21].

Therefore, we propose hydrogels as a good alternative for EV formulation and clinical application to overcome direct titanium functionalization and achieve a smother translation to the orthopedical field. HA is an extracellular component that modulates tissue regeneration [22]. Moreover, HA gels have been previously used for cell-derived EV encapsulation in bone healing applications [23]. In previous studies, we have combined HA gels with pEVs showing improvements *in vitro* for gingival regeneration [24]. Even more, gels without EVs have already been applied on titanium implants in order to improve the osteointegration and biocompatibility of the bone grafts [25]. Thus, EV formulated HA gels could benefit any implantable material given its ease of applicability to different implants.

To sum up, despite the evidences that support the clinical use of pEVs in the orthopaedical or periodontal field, only few studies have evaluated their effect *in vivo* [10,26]. Hence, in this study, we aim to further study the local effects of pEVs in a rabbit model by applying pEV functionalized HA gels at the bone defect before implantation in order to achieve their effective translation to the clinics. Overall, understanding the role of pEVs *in vivo* could ease their future use in bone healing therapies in the clinical field.

2. Materials and methods

2.1. PL preparation and EV isolation

The current project was approved by the IdISBa Biobank Ethics Committee (IB 1995/12 BIO). Platelet Lysate (PL) was obtained as previously described [9]. Briefly, fresh buffy coats were obtained from the IdISBa Biobank and pulled. After 10 min of centrifugation at 650×*g* and leucocyte filtration, platelet concentrates were obtained. Then, at least three freeze/thaw cycles at −80 °C and 37 °C were performed, large cell debris were discarded by centrifugation at 5050×*g* for 20 min and filtration through 40.0 µm pore size membrane (Sartorius, Goettingen, Germany). PL was stored at −20 °C until use.

For EV isolation, PL was centrifuged for 15 min at 1500×*g*. The supernatant was filtered, first through 0.8 µm and then 0.2 µm porous membranes (Sartorius). PL was centrifuged at 10,000×*g* for 30 min and 5 ml were loaded on a Sepharose CL-2B precast column (GE Healthcare, Pittsburg, PA, USA). AKTA purifier system coupled with a collector Frac 950 (GE Healthcare) was set at 0.5 ml/min flow rate. EVs were eluted with PBS (Capricorn, Ebsdorfergrund, Germany) in 5 ml fractions. Then, pEVs were concentrated using spin filters with a pore size of 100 kDa (Pall Corporation, Port Washington, NY, USA). Centrifugation steps at 5000×*g* were repeated until the volume of EVs did not decrease anymore. EVs were stored at – 80 °C until use.

EVs isolated using identical protocols and the same settings have been repeatedly characterised for morphology, total protein amounts and CD9 and CD63 presence in our previous publications [9,20,24]. In those studies, the vesicular nature of the EVs and the EV specific markers were confirmed following the criteria of the MISEV 2018 guidelines [21].

2.2. Hydrogel preparations

Hyaluronic acid (HA; Bioibérica, F002103, Mw 800–1200 kDa, Spain) gels were prepared at 2% concentration. HA was resuspended with the EV sample, achieving the highest concentration possible ($6{\cdot}10^{11}$ part/ml), or in PBS as a control group (C), by overnight incubation at room temperature.

2.3. Implants and animal surgery

Coin-shaped grade 2 titanium implants were used. Implants presented a diameter of 6.25 mm and a height of 1.95 mm. The test surfaces were blasted with titanium dioxide (TiO_2) particles to surface roughness of Sa = 1.5 μm [27]. All implants were washed [28] and sterilized by UV-irradiation.

Eight healthy 20 weeks old male adult New Zealand White rabbits, that weighted around 4.8–5.2 kg, were used in this *in vivo* study. The experiments had been approved and registered by Universidad de Santiago de Compostela Ethics Committee (06/18/LU-002) and were conducted following the Spanish and European Union regulations about care and use of research animals. Detailed information regarding the surgery and anaesthetic protocol has already been published previously [29]. Briefly, an incision was made on the proximal-anterior part of each tibia that allowed the exposure of the underlying periosteum and its removal. Then, two holes in each leg were made with a twist drill (Medicons, Germany) with copious physiological saline solution irrigation to avoid overheating. The implants were retained in the cortical bone with a titanium band and two titanium screws (Medicons CMS, Germany). This ensured a stable initial fixation of the implants during the healing period. Polytetrafluoroethylene (PTFE) caps were placed on the opposite side of the implants to inhibit bone growth towards the vertical parts and on the backside of the implants to allow biomechanical testing.

For each animal, one leg was treated with HA and was used as the Control group, while the other leg was treated with HA-EVs and set as the treatment group. Left and right leg were alternatively assigned to control or treatment. The animals were kept in individual cages for eight weeks in a controlled environment, with food and water ad libitum and environmental enrichment. Health status of the animals was daily monitored by accredited veterinarians trained in laboratory animal science. Half of the rabbits were destined to histological and micro-computed tomography (micro-CT) analyses (n = 8), while the other four rabbits were used for the biomechanical test and molecular biology analyses (n = 8). Fig. 1 details the animal model set-up. The experiments and data analyses were conducted in a blinded fashion.

2.4. Tensile test

Eight weeks after the surgery, the bone-to-implant attachment strength was evaluated using the pull-out removal tensile test. For some samples, implants were lost during manipulation for the removal of the teflon caps, and biomechanical test could not be performed on them. A material testing machine (MicroTest, Madrid, Spain) fitted with a calibrated load-cell of 1 kN was used. Cross-head speed range was set to 1.0 mm/min. The maximum applied load before the implant detached from the bone was recorded. Detailed information regarding the pull-out test has already been published previously [29].

After extracting the coins, the implants were placed in a Tripure solution and stored until RNA extraction. The remaining wound fluid was collected by applying a filter paper in the bone defect for 1 min. Then, the impregnated paper was transferred into 200 μl PBS solution and placed on ice, until the biochemical analyses were performed.

2.5. Wound fluid analyses: Total protein determination, LDH activity and ALP activity

Wound fluid total protein was analysed spectrophotometrically using Nanodrop 2000 (Thermo Fisher) at λ = 280 nm. Lactate dehydrogenase (LDH) activity was measured with Cytotoxicity Detection kit (Roche Diagnostics, Manheim, Germany). Samples were incubated for 30 min at room temperature, and they were read at λ = 490 nm, by measuring NADH oxidation in pyruvate presence.

For alkaline phosphatase (ALP) activity, samples were incubated with 100 μl of p-Nitrophenyl Phosphate (Sigma–Aldrich) for 2 h at 37 °C. In parallel, a standard curve was prepared using calf intestinal ALP (Promega, Madison, WI, USA). The p-Nitrophenyl Phosphate end product induced by the ALP activity absorbs at λ = 405 nm and was used to quantify ALP activity.

Table 1
Genes and sense (S) and antisense (A) primers used in gene expression analysis.

Gene	Primer sequence (5'→3')	Amplicon size (bp)	Function
Osteocalcin (*Oc*)	S: CTTCGTGTCCAAGAGGGAGG A: CTCCAGGGGATCCGGGTAA	100	Target gene: bone formation
Runt-related transcription factor 2 (*Runx2*)	S: GCCTTCAAGGTGGTAGCCC A: CGTTACCCGCCATGACAGTA	67	Target gene: bone formation
Collagen type I (*Coll-I*)	S: AGAGCATGACCGATGGATTC A: CCTTCTTGAGGTTGCCAGTC	177	Target gene: bone formation
Bone morphogenetic protein 2 (*Bmp-2*)	S: ATGGGTTTGTGGTGGAAGTG A: GCTGTTTGTGTTTCGCTTGA	195	Target gene: bone formation
Tartrate-resistant acid phosphatase (*Trap*)	S: CCTGGGCGACAACTTTTACT A: TTGGAGACCTTGGAATAGGC	180	Target gene: bone resorption
Calcitonin receptor (*Calcr*)	S: CAAATGACACCCATCCAACA A: ACATCCATCCATCCCAGGTC	162	Target gene: bone resorption
Proton ATPase (*H + ATPasa*)	S: CCGAAACCTCCTGAAGAAAA A: ATAGCCGTGGTGCTGAAGTC	165	Target gene: bone resorption
Receptor activator of nuclear factor-kappaB ligand (*Rankl*)	S: CAGAGCGCAGATGGATCCTAA A: TCCTTTTGCACAGCTCCTTGA	180	Target gene: bone resorption
18s ribosomal RNA	S: GTAACCCGTTGAACCCCATT A: CCATCCAATCGGTAGTAGCG	151	Reference gene
Glyceraldehyde-3-phosphate dehydrogenase	S: TGCACCACCAACTGCTTAGC A: GGCATGGACTGTGGTCATGAG	87	Reference gene
Beta-actin	S: GCGACCTCACCGACTACC T A: GCCATCTCGTTCTCGAAGTC	136	Reference gene

2.6. RNA isolation and real-time RT-PCR

RNA was isolated from the peri-implant bone tissue attached to the extracted implants using Tripure Isolation Reagent (Roche Diagnostics), according to the manufacturer's protocol. RNA concentration was determined by the NanoDrop spectrophotometer at 260 nm. RNA amount was normalized for reverse transcription to cDNA using High Capacity RNA-to-cDNA kit (Applied Biosystems, Foster City, CA, USA).

Real-time PCR was performed for reference genes and target genes (Table 1) using the Lightcycler 480 thermocycler (Roche Diagnostics). Each reaction well contained Lightcycler 480 SYBR Green I Master (Roche Diagnostics), the cDNA sample and 0.5 μM of each primer, the sense and the antisense, in a final volume of 10 μl. The amplification program started with 5 min denaturation step for cDNA at 95 °C, followed by 45 cycles consisting of denaturation at 95 °C, annealing at 60 °C and an extension at 72 °C. Fluorescence was measured at 72 °C after each

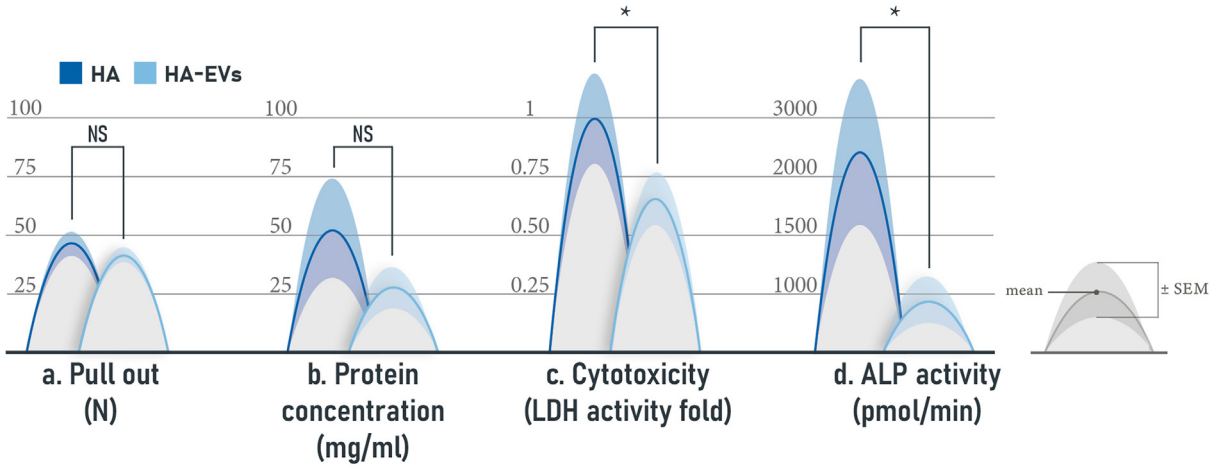

Fig. 2. Cytotoxicity and osteointegration in the wound fluid. (a) Pull-out force required for implants extraction (n = 6, since 2 samples were lost during the extraction process). **(b)** Protein concentration in the wound fluid after implant extraction (n = 8). **(c)** LDH activity in the wound fluid. LDH activity was normalized respect to the HA group that was set to 1 (n = 8). **(d)** ALP activity in the wound fluid (n = 8). Data represents the mean value ± SEM. In addition, paired data points are connected by a straight line between HA and HA-EV groups. For statistical analysis, paired t-test were performed and $p < 0.05$ were considered statistically significant and represented with *.

cycle. Standard curves were constructed for relative quantification. The Second Derivative Maximum Method provided by the LightCycler480® analysis software version 1.5 (Roche Diagnostics) was used to calculate the amount of each gene from the crossing point data. Reference genes were used to normalize the target genes expressions levels and changes were compared to Control group, which was set to 100%.

2.7. Micro-CT analysis

Samples for analysis were fixated in 4% formaldehyde and then kept in 70% ethanol. A high-resolution micro-CT (Skyscan 1172, Bruker microCT NV, Kontig, Belgium) was used to scan the samples. The X-ray source was set at 100 kV and 100 μA with a pixel size of 8 μm (camera binning 2 × 2) and the use of an Aluminium 0.5 mm filter. The sample scan was performed with a 360° rotation and images were acquired every 0.4°. Then, images were reconstructed using NRecon software (Bruker microCT NV) and evaluated with the DataViewer software (Bruker microCT NV) to place the implant completely parallel to the y axis. Later, the transaxial images were loaded in CTAn software (Bruker microCT NV) and a VOI up to 50 μm from the bottom of the metallic implant was recorded. The volume defined from the bottom to the 50 μm layer was defined as the total tissue volume. The threshold level was set in 35–255. The analysis was performed, and different parameters were evaluated, including the bone-to-implant contact (BIC), the bone volume over the tissue volume (BV/TV) and the bone surface over the bone volume (BS/BS).

2.8. Histological analysis

Samples were dehydrated in ascending ethanol concentrations and embedded in a photopolymerizable glycol metacrylate resin (Technovit 7200 VLC, Heraeus-Kulzer, Wehrheim, Germany). Then, the polymerized tissue blocks were cut and polished with the Exakt equipment (Exakt Apparatebau GMBH, Norderstedt, Germany). Central sections with 40 μm of thickness were stained by Levai-Laczkó's protocol and imaged with an Olympus BX51 microscope (Olympus Corporation, Tokyo, Japan). Whole section images were taken at 4 × augments, while close-up images near the implant region were captured at 10 × augments.

Images were analyzed to determine the BIC using the Olympus Cell-sens 1.5 (Olympus Corporation). Moreover, the stained images were colored with Adobe Photoshop CS6 (Adobe Systems Incorporated, San Jose, USA), distinguishing new bone tissue (pink) from pristine bone (non-colored) and soft tissue (white). The studied areas were defined up to 100 μm from the implant and measured with Olympus Cell-sens 1.5 to determine the percentage area of new bone and the number of blood vessels in the peri-implant region. The implants were evaluated according to UNE-EN ISO 10993–6 as previously described [30].

2.9. Statistical analysis

For statistical analysis, SPSS program version 27.0 (SPSS Inc., Chicago, IL, USA) was used. Paired t-test comparison was performed to evaluate statistical differences. For qualitative data, chi-square test was performed. Results were considered significant at $p < 0.05$. Graphs show mean values and the standard error of the mean.

2.10. Approval of ethics committee

The project use of human PL was approved by the IdISBa Biobank Ethics Committee (IB 1995/12 BIO). All persons involved had provided their informed consent prior to inclusion in the study and the European Medicines Agency Guidelines for Good Clinical Practice was applied. Moreover, the animal experiments had been approved and registered by Universidad de Santiago de Compostela Ethics Committee (06/18/LU-002) and were conducted following the Spanish and European Union regulations about care and use of research animals.

3. Results

3.1. Biomechanical test and biochemical analyses of the wound fluid

First, functional effects of pEV treatments at the Ti implant interface were evaluated through the biomechanical test and the biochemical analysis of the wound fluid after the implant removal (Fig. 2). On the one hand, no significant difference was observed in terms of the pull-out force. On the other hand, there was a decreasing tendency in the protein amount in the wound fluid of HA-EV treated group, despite not reaching statistical significance, while LDH and ALP activity were significantly decreased in the HA-EV treated group compared to the control group.

3.2. Gene expression of bone markers at the bone-implant interface

Then, mRNA expression of bone marker genes by the tissue attached

Table 2
Gene expression effects on the peri-implant region. Gene expression for HA group was normalized and set to 100%. Data represents de mean value ± SEM (n = 8). Data was compared with paired-t-test analysis.

gene		*mRNA expression levels (%)*		*p-value*
		HA	HA-EVs	
Bone formation	*Bmp-2*	100 ± 4.0	91.2 ± 5.4	0.276
	Coll-1	100 ± 3.5	98.0 ± 7.8	0.697
	Oc	100 ± 3.1	103.2 ± 4.4	0.521
	Runx2	100 ± 9.2	152.0 ± 39.5	0.254
Bone resorption	*Calcr*	100 ± 4.2	104.5 ± 10.1	0.758
	H + ATPase	100 ± 2.6	93.4 ± 4.6	0.190
	Rankl	100 ± 2.9	103.0 ± 3.9	0.424
	Trap	100 ± 2.5	104.3 ± 3.0	0.264

on the implants was evaluated (Table 2). Osteogenic genes such as *Bmp-2, Coll-I, Oc* and *Runx2* showed no significant difference, although *Runx2* presented a 1.7-fold higher mean value for the treated group compared to the control, despite not reaching statistical significance. Bone resorption related genes such as *Trap, Calcr, Rankl* and *H + ATPase* did not present any statistical difference either.

3.3. Micro-CT and histological analyses

After that, micro-CT analysis were performed to determine bone-to-implant contact and other bone morphometric parameters in the volume of interest (Fig. 3). Representative images for both groups (HA and HA-EVs) show the location of the implant area in the tibia. 3D reconstructed images can be visualized in the following database link: 10.6084/m9. figshare.22,734,581. However, no differences were found on the micro-CT analysis of the bone at the implant interface. Nevertheless, a tendency to higher values of BV/TV and lower values of BS/BV for the HA-EV group than the control HA group were observed, despite not reaching statistical significance.

Finally, histological analyses were performed to evaluate bone histomorphometry and local effects after implantation following UNE-EN ISO 10993–6:2017 (Fig. 4). Representative images for both groups show representative cross-sections in which calcified regions are pinkish, while nucleus and cytoplasm are visualized in blue. Furthermore both, treatments present absent or slight irritative affects according to the UNE-EN ISO 10993–6:2017 evaluation and only the fibrosis levels were significantly lower for HA-EV treated group, compared to the HA control. Nonetheless, the global score was not significantly different, despite the lower value of HA-EV treated group. In addition, the histological analysis confirmed that no differences were appreciable in terms of BIC values. However, HA-EV treated samples showed an increased number of blood vessels count and presented a higher percentage of new bone area, despite not reaching statistically significant p values.

4. Discussion

In this study, HA gels formulated with pEVs showed an improvement in terms of biocompatibility and tissue response that could allow their future translation to clinics. Biochemical analyses of the wound fluid and tissue analyses show a decrease in tissue necrosis and fibrosis in the peri-implant region. Moreover, bone healing indicators, such as ALP activity, bone volume over tissue volume and the percentage of new bone suggest a further advanced stage of regeneration. Therefore, pEV HA gels seem to

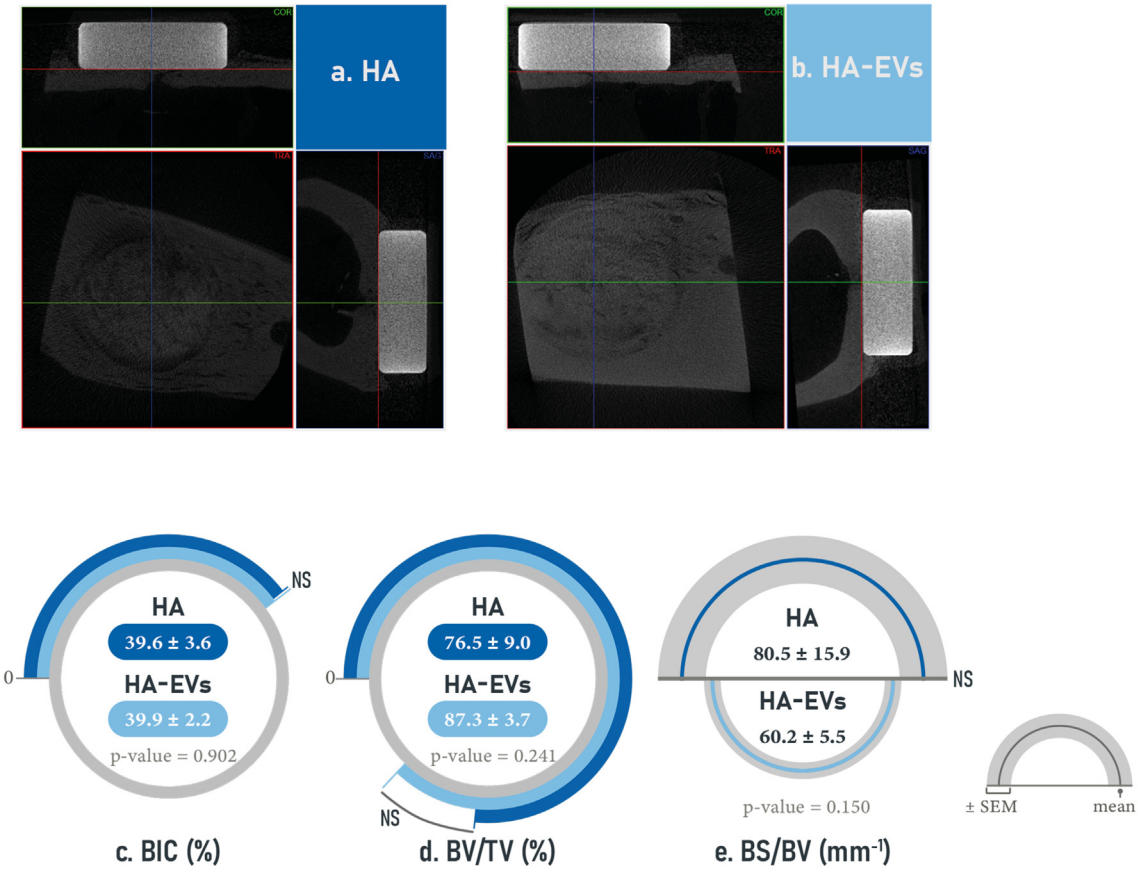

Fig. 3. Representative images and analysis of micro-CT implant to a depth of 50 µm. (a) Representative images of the micro-CT bone-implant for the HA treated group. **(b)** Representative images of the micro-CT bone-implant for the HA-EVs treated group. **(c)** Main values obtained from the images analysis including bone-to-implant contact (BIC), **(d)** bone volume over tissue volume (BV/TV) and **(e)** bone surface over bone volume (BS/BV). Data represents de mean value ± SEM (n = 8) and it was statistically compared by paired t-test.

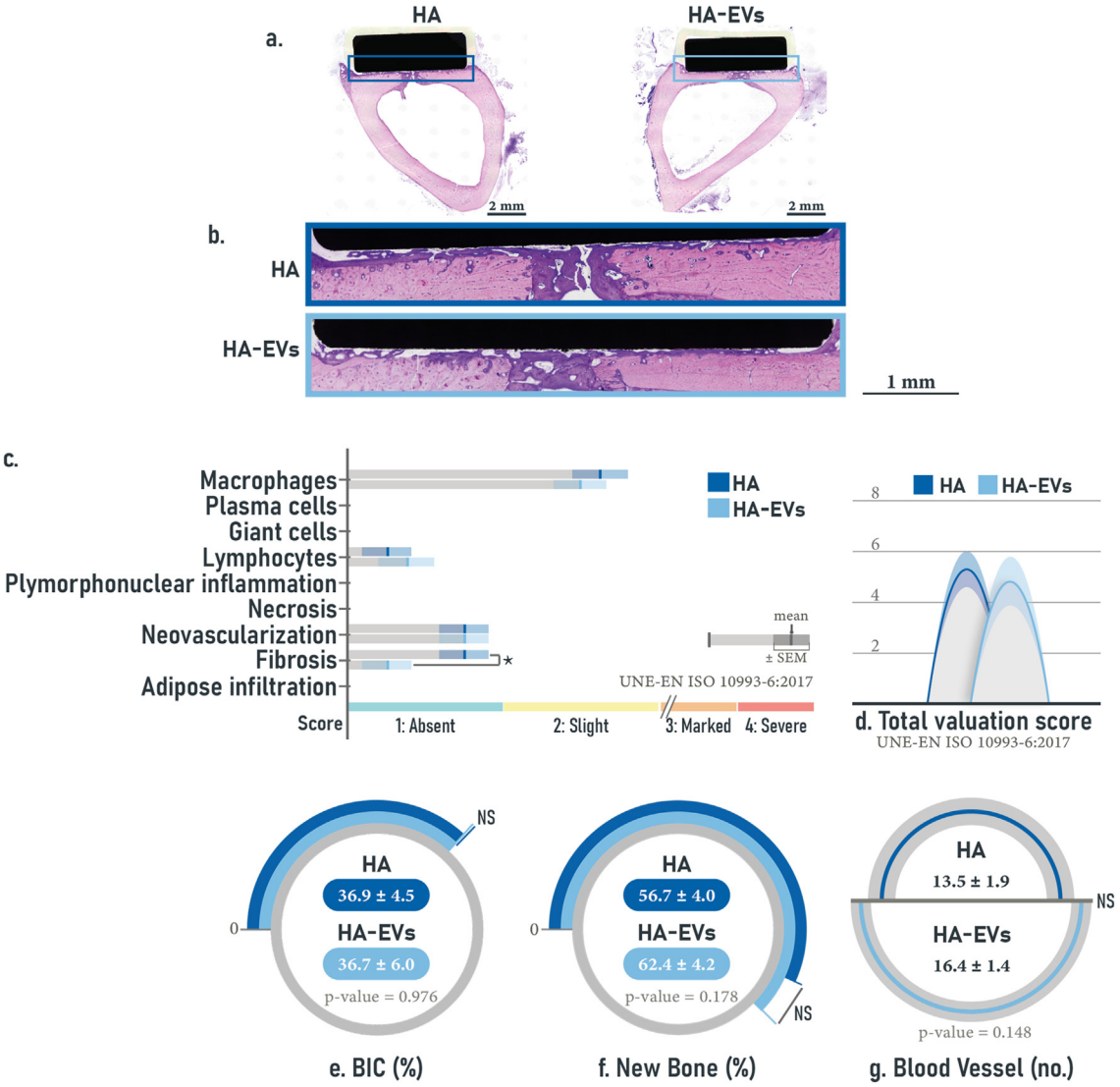

Fig. 4. Histological evaluation of HA-EV and HA treated implant sections. (a) Representative histological sections at 4 × augments near the central region of the implant. **(b)** Close-up representative histological sections at 10 × augments at the bone-implant area. **(c)** UNE-EN ISO 10993–6:2017 evaluation of the different parameters and their respective scores, being 0 equal to absent, 1 slight, 2 moderate, 3 marked and 4 severe. Data represents de mean value ± SEM (n = 8) and it was compared throw chi-squared test. P < 0.05 were considered statistically significant and represented with *. **(d)** Total UNE-EN ISO 10993–6:2017 evaluation score. **(e)** Main values obtained from the images analysis including bone-to-implant contact (BIC), **(f)** new bone formation and **(g)** blood vessel number. Data represents de mean value ± SEM (n = 8) and it was statistically compared by paired t-test.

be good candidates for improving bone healing and being used in the orthopaedical field.

First, the obtained results indicate that pEV-HA treated implants present an improved biocompatibility compared to HA group. Biochemical determination of LDH activity and protein concentration was decreased in pEV treated groups. LDH is a cytoplasmic enzyme that is released to the extracellular space due to cell lysis. Therefore, its presence in the wound fluid can be related to the necrotic processes induced by the surgery and implantation [31]. The decrease of LDH activity in pEV treated implants agrees with a previous study which demonstrated that pEVs prevented apoptosis in a rat osteonecrotic model [10]. Moreover, protein concentration was slightly lower in pEV treated implants, indicating that the blood clotting process had also diminished, and that the inflammation stage of bone healing was leading to new bone tissue formation [32].

In addition, histological samples were evaluated according to ISO 10993–6:2017 for implantable materials and none of the treatments, HA gels nor pEV formulated HA gels, supposed an irritative effect. Therefore, both treatments are highly safe, even that pEV formulated gels show slightly better biocompatibility. In fact, among the different parameters evaluated, fibrosis was significantly lower in pEV formulated gels compared to HA gels, although in both cases only narrow or no band of fibrosis were observed since they both had low scores for fibrosis parameter. These findings are not surprising, since HA is already known to be an excellent candidate for bone healing, promoting osteoblasts recruiting and scarless wound regeneration when used to functionalize titanium implants [33]. The fact that HA already presents these regenerative characteristics may have hide some of the positive effects of pEVs, since HA for itself is already promoting bone healing [33]. Thus, the evaluation of non-formulated pEVs remains as a limitation of our study. Nonetheless, according to our results, pEVs are able to even improve these regenerative properties, which are especially important to avoid the foreign body reaction and the encapsulation of the implants through a fibrotic tissue [34]. Therefore, by diminishing the fibrosis effect, pEVs are also avoiding implant failure and enhancing bone regeneration through direct interaction of the implants with the bone tissue.

In terms of bone regeneration, pEVs also present improvements in the regenerative stage in which the tissue is found. Although there were no differences for mRNA expression, *Runx2* levels were slightly higher for pEV treated groups. RUNX2 is a transcription factor that up-regulates different genes, including bone sialoprotein, *Oc* and *Col1a1*, which lead to osteoblast differentiation [35]. In previous *in vitro* studies, performed on mesenchymal stem cells, *Runx2* mRNA levels were significantly higher when treated with pEVs [9]. However, here, statistical significance was not reached, probably due to the higher complexity of the animal model compared to cell culture. Despite the lack of evidence in gene expression of the bone attached to the implant after the pull out test, ALP activity in pEV treated implants was significantly lower. ALP has a bone mineralization role during the first stages of calcification, thus, it can be used as an early marker of osteoblast differentiation [36]. Therefore, lower levels of ALP activity after the eight weeks of the surgical intervention indicate that pEV treated implants have already surpassed these early stages of bone healing and they are in a more mature mineralization phase. In fact, previous studies demonstrated that there is a negative correlation between the pull-out force and ALP activity, therefore ALP lower levels can be associated to a further implant healing which have already overcome the primary mineralization stage [32]. In addition, the low levels of protein concentration in the wound fluid of the pEV treated group is also related to bone mineralization, since low levels of protein are associated to more mature bone tissue healing stages [37]. After the blood clot around the implant is organized, it is replaced by new tissue, therefore, the wound fluid total protein is negatively correlated to the binding between the implant and the bone [32].

Furthermore, these biochemical changes are also related to micro-CT and histological results. The increase in BV/TV, despite not being statistically significant, indicates a higher bone formation at the volume of interest, surrounding the implant interface. In fact, BV/TV ratio is known to be negatively correlated to BS/BV ratio [38], in agreement with the lower BS/BV, along with higher BV/TV shown for the EV-HA group. The regenerative process is also reflected in the histology values of number of blood vessels and new bone formation. In fact, some studies had already suggested that pEVs induce neovascularization in the peri-implant region [26]. Although statistical differences were not reached for the number of blood vessels, increased values were determined for pEV treated implants. Nonetheless, probably higher pEV treatment doses might be needed to reach more robust *in vivo* results.

Overall, here we show that pEVs are able to induce biocompatibility improvements of Ti implants and to stimulate tissue remodelling. However, these changes are not translated into improved bone-to-implant contact nor biomechanical properties. In addition, in spite of the tendencies observed, differences in the mineralization and biochemical parameters are not always statistically significant. It is important to acknowledge that small sample size can limit the statistical power of the study and affect the extrapolation of the findings. Nonetheless, the results suggest that pEVs contribute to the bone healing effects, not only by diminishing the necrotic process, but also by improving the angiogenesis, the bone remodelling and also preventing fibrous tissue formation around the implant. In future studies, crosslinked gels or higher molecular weight HA molecules could be evaluated in order to improve the sustained release, and thus, the positive effects of pEVs on bone regeneration [39].

Finally, it is worth mentioning that there is still little bibliography around pEV effects *in vivo*. In fact, most EV research is still focused on mesenchymal stem cells [40]. Stem cells are widely diverse, and the cell culture growth and expansion hinder their use in clinics [41]. On the contrary, we and others have shown regenerative properties of platelet derived EVs, and, what is more, their translation to the clinics presents some advantages, since clinical-grade allogenic platelets are already obtained from whole-blood donations, and pEVs are isolated without further cell expansion, altogether allowing a faster translation for their use [41]. Therefore, here we propose pEVs as an alternative treatment for bone regeneration.

5. Conclusions

In conclusion, pEVs formulated with HA have shown to improve biocompatibility at the bone implant interface, since they diminish the fibrosis and necrosis in the peri-implant region. Further studies should be performed to assess the robustness of our findings, and to reach statistical significances in terms of osteogenesis and angiogenesis after 8 weeks of healing in this *in vivo* model. However, our results indicate that the orthopaedical field could benefit from the use of pEVs.

Declaration of competing interest

All authors declare no conflict of interests.

Acknowledgements

This research was funded by Instituto de Salud Carlos III, co-funded by the ESF European Social Fund and the ERDF European Regional Development Fund (contract to J.M.R; MS16/00124 and projects PI17/01605 and PI20/00127) and the Direcció General d'Investigació, Conselleria d'Investigació, Govern Balear (contract to M.A.R.; FPI/2046/2017) and the Institut d'Investigació Sanitària de les Illes Balears (contract to M.A.F.G; ITS2018-002-TALENT PLUS JUNIOR PROGRAM, JUNIOR18/01). The authors thank SCT-UIB for access to their facilities and the IdISBa Biobank for providing the PL. The authors are grateful to Illustrate Science (http://www.illustrate-science.com/) for assistance with the Figures. The authors state there are no conflict of interests.

References

[1] Phan TH, Kim SY, Rudge C, Chrzanowski W. Made by cells for cells - extracellular vesicles as next-generation mainstream medicines. J Cell Sci 2022;135. https://doi.org/10.1242/jcs.259166.
[2] Veerman RE, Güçlüler Akpinar G, Eldh M, Gabrielsson S. Immune cell-derived extracellular vesicles - functions and therapeutic applications. Trends Mol Med 2019;25:382–94. https://doi.org/10.1016/j.molmed.2019.02.003.
[3] Girón J, Maurmann N, Pranke P. The role of stem cell-derived exosomes in the repair of cutaneous and bone tissue. J Cell Biochem 2022;123:183–201. https://doi.org/10.1002/jcb.30144.
[4] Everts P, Onishi K, Jayaram P, Lana JF, Mautner K. Platelet-Rich plasma: new performance understandings and therapeutic considerations in 2020. Int J Mol Sci 2020;21:1–36. https://doi.org/10.3390/ijms21207794.
[5] Samadi P, Sheykhhasan M, Khoshinani HM. The use of platelet-rich plasma in aesthetic and regenerative medicine: a comprehensive review. Aesthetic Plast Surg 2019;43:803–14. https://doi.org/10.1007/s00266-018-1293-9.
[6] Wu PIK, Diaz R, Borg-Stein J. Platelet-Rich plasma. Phys Med Rehabil Clin 2016;27:825–53. https://doi.org/10.1016/j.pmr.2016.06.002.
[7] Wu J, Piao Y, Liu Q, Yang X. Platelet-rich plasma-derived extracellular vesicles: a superior alternative in regenerative medicine? Cell Prolif 2021;54:e13123. https://doi.org/10.1111/cpr.13123.
[8] Torreggiani E, Perut F, Roncuzzi L, Zini N, Baglìo SR, Baldini N. Exosomes: novel effectors of human platelet lysate activity. Eur Cell Mater 2014;28:137–51. https://doi.org/10.22203/ecm.v028a11. ; discussion 151.
[9] Antich-Rosselló M, Forteza-Genestra MA, Calvo J, Gayà A, Monjo M, Ramis JM. Platelet-derived extracellular vesicles promote osteoinduction of mesenchymal stromal cells. Bone Jt Res 2020;9:667–74. https://doi.org/10.1302/2046-3758.910.BJR-2020-0111.R2.
[10] Tao S-C, Yuan T, Rui B-Y, Zhu Z-Z, Guo S-C, Zhang C-Q. Exosomes derived from human platelet-rich plasma prevent apoptosis induced by glucocorticoid-associated endoplasmic reticulum stress in rat osteonecrosis of the femoral head via the Akt/Bad/Bcl-2 signal pathway. Theranostics 2017;7:733–50. https://doi.org/10.7150/thno.17450.
[11] Ferreira MR, Zambuzzi WF. Platelet microparticles load a repertory of miRNAs programmed to drive osteogenic phenotype. J Biomed Mater Res 2020. https://doi.org/10.1002/jbm.a.37140.
[12] Puhm F, Boilard E, MacHlus KR. Platelet extracellular vesicles: beyond the blood. Arterioscler Thromb Vasc Biol 2020;87–96. https://doi.org/10.1161/ATVBAHA.120.314644.
[13] Brill A, Dashevsky O, Rivo J, Gozal Y, Varon D. Platelet-derived microparticles induce angiogenesis and stimulate post-ischemic revascularization. Cardiovasc Res 2005;67:30–8. https://doi.org/10.1016/j.cardiores.2005.04.007.
[14] Li Y, Yang C, Zhao H, Qu S, Li X, Li Y. New developments of Ti-based alloys for biomedical applications. Materials 2014;7:1709–800. https://doi.org/10.3390/ma7031709.
[15] Pansani TN, Phan TH, Lei Q, Kondyurin A, Kalionis B, Chrzanowski W. Extracellular-vesicle-based coatings enhance bioactivity of titanium implants-SurfEV. Nanomaterials 2021;11:1445. https://doi.org/10.3390/nano11061445.

[16] Chen L, Mou S, Li F, Zeng Y, Sun Y, Horch RE, et al. Self-assembled human adipose-derived stem cell-derived extracellular vesicle-functionalized biotin-doped polypyrrole titanium with long-term stability and potential osteoinductive ability. ACS Appl Mater Interfaces 2019;11:46183–96. https://doi.org/10.1021/acsami.9b17015.
[17] Chen L, Mou S, Hou J, Fang H, Zeng Y, Sun J, et al. Simple application of adipose-derived stem cell-derived extracellular vesicles coating enhances cytocompatibility and osteoinductivity of titanium implant. Regen Biomater 2021;8:1–9. https://doi.org/10.1093/rb/rbaa038.
[18] Wei F, Li M, Crawford R, Zhou Y, Xiao Y. Exosome-integrated titanium oxide nanotubes for targeted bone regeneration. Acta Biomater 2019;86:480–92. https://doi.org/10.1016/j.actbio.2019.01.006.
[19] Zhao Q, Zhang Y, Xiao L, Lu H, Ma Y, Liu Q, et al. Surface engineering of titania nanotubes incorporated with double-layered extracellular vesicles to modulate inflammation and osteogenesis. Regen Biomater 2021;8:rbab010. https://doi.org/10.1093/rb/rbab010.
[20] Antich-Rosselló M, Forteza-Genestra MA, Calvo J, Gayà A, Monjo M, Ramis JM. Customizing the extracellular vesicles release and effect by strategizing surface functionalization of titanium. Sci Rep 2022;12:7399. https://doi.org/10.1038/s41598-022-11475-3.
[21] Théry C, Witwer KW, Aikawa E, Alcaraz MJ, Anderson JD, Andriantsitohaina R, et al. Minimal information for studies of extracellular vesicles 2018 (MISEV2018): a position statement of the International Society for Extracellular Vesicles and update of the MISEV2014 guidelines. J Extracell Vesicles 2018;7:1535750. https://doi.org/10.1080/20013078.2018.1535750.
[22] Graça MFP, Miguel SP, Cabral CSD, Correia IJ. Hyaluronic acid—based wound dressings: a review. Carbohydr Polym 2020;241:116364. https://doi.org/10.1016/j.carbpol.2020.116364.
[23] Zhang Y, Xie Y, Hao Z, Zhou P, Wang P, Fang S, et al. Umbilical mesenchymal stem cell-derived exosome-encapsulated hydrogels accelerate bone repair by enhancing angiogenesis. ACS Appl Mater Interfaces 2021;13:18472–87. https://doi.org/10.1021/acsami.0c22671.
[24] Antich-Rosselló M, Munar-Bestard M, Forteza-Genestra MA, Calvo J, Gayà A, Monjo M, et al. Evaluation of platelet-derived extracellular vesicles in gingival fibroblasts and keratinocytes for periodontal applications. Int J Mol Sci 2022;23:7668. https://doi.org/10.3390/ijms23147668.
[25] Kotlarz M, Ferreira AM, Gentile P, Dalgarno K. Bioprinting of cell-laden hydrogels onto titanium alloy surfaces to produce a bioactive interface. Macromol Biosci 2022;22:e2200071. https://doi.org/10.1002/mabi.202200071.
[26] Moest T, Koehler F, Prechtl C, Schmitt C, Watzek G, Schlegel KA. Bone formation in peri-implant defects grafted with microparticles: a pilot animal experimental study. J Clin Periodontol 2014;41:990–8. https://doi.org/10.1111/jcpe.12295.
[27] Monjo M, Lamolle SF, Lyngstadaas SP, Rønold HJ, Ellingsen JE. In vivo expression of osteogenic markers and bone mineral density at the surface of fluoride-modified titanium implants. Biomaterials 2008;29:3771–80. https://doi.org/10.1016/j.biomaterials.2008.06.001.
[28] Antich-Rosselló M, Forteza-Genestra MA, Calvo J, Gayà A, Monjo M, Ramis JM. Platelet-derived extracellular vesicle functionalization of Ti implants. JoVE. JoVE 2021:e62781. https://doi.org/10.3791/62781.
[29] Rønold HJ, Ellingsen JE. The use of a coin shaped implant for direct in situ measurement of attachment strength for osseointegrating biomaterial surfaces. Biomaterials 2002;23:2201–9. https://doi.org/10.1016/s0142-9612(01)00353-2.
[30] Velasco-Ortega E, Ortiz-García I, Jiménez-Guerra A, Monsalve-Guil L, Muñoz-Guzón F, Perez RA, et al. Comparison between sandblasted acid-etched and oxidized titanium dental implants: in vivo study. Int J Mol Sci 2019;20. https://doi.org/10.3390/ijms20133267.
[31] Williams DL, Marks V, editors. Biochemistry in clinical practice. London: Heinemann; 1983.
[32] Monjo M, Ramis JM, Rønold HJ, Taxt-Lamolle SF, Ellingsen JE, Lyngstadaas SP. Correlation between molecular signals and bone bonding to titanium implants. Clin Oral Implants Res 2013;24:1035–43. https://doi.org/10.1111/j.1600-0501.2012.02496.x.
[33] Cervino G, Meto A, Fiorillo L, Odorici A, Meto A, D'Amico C, et al. Surface treatment of the dental implant with hyaluronic acid: an overview of recent data. Int J Environ Res Publ Health 2021;18. https://doi.org/10.3390/ijerph18094670.
[34] Klopfleisch R, Jung F. The pathology of the foreign body reaction against biomaterials. J Biomed Mater Res, Part A 2017;105:927–40. https://doi.org/10.1002/jbm.a.35958.
[35] Loebel C, Czekanska EM, Bruderer M, Salzmann G, Alini M, Stoddart MJ. In vitro osteogenic potential of human mesenchymal stem cells is predicted by Runx2/Sox9 ratio. Tissue Eng 2015;21:115–23. https://doi.org/10.1089/ten.TEA.2014.0096.
[36] Golub EE, Harrison G, Taylor AG, Camper S, Shapiro IM. The role of alkaline phosphatase in cartilage mineralization. Bone Miner 1992;17:273–8. https://doi.org/10.1016/0169-6009(92)90750-8.
[37] Sodek KL, Tupy JH, Sodek J, Grynpas MD. Relationships between bone protein and mineral in developing porcine long bone and calvaria. Bone 2000;26:189–98. https://doi.org/10.1016/s8756-3282(99)00251-3.
[38] Xie F, Zhou B, Wang J, Liu T, Wu X, Fang R, et al. Microstructural properties of trabecular bone autografts: comparison of men and women with and without osteoporosis. Arch Osteoporosis 2018;13:18. https://doi.org/10.1007/s11657-018-0422-z.
[39] Bayer IS. Hyaluronic acid and controlled release: a review. Molecules 2020;25. https://doi.org/10.3390/molecules25112649.
[40] Murali VP, Holmes CA. Mesenchymal stromal cell-derived extracellular vesicles for bone regeneration therapy. BoneKEy Rep 2021;14:101093. https://doi.org/10.1016/j.bonr.2021.101093.
[41] Johnson J, Wu Y-W, Blyth C, Lichtfuss G, Goubran H, Burnouf T. Prospective therapeutic applications of platelet extracellular vesicles. Trends Biotechnol 2021;39:598–612. https://doi.org/10.1016/j.tibtech.2020.10.004.